Metatarsal Loading During Gait—A Musculoskeletal Analysis

Amir A. Al-Munajjed[1]
Musculoskeletal Research,
Anybody Technology,
Niels Jernes Vej 10,
Aalborg 9220, Denmark
e-mail: amir.al-munajjed@gmx.de

Jeffrey E. Bischoff
Research and Development,
Zimmer, Inc.,
Warsaw, IN 46581

Mehul A. Dharia
Research and Development,
Zimmer, Inc.,
Warsaw, IN 46581

Scott Telfer
Institute of Applied Health Research,
Glasgow Caledonian University,
Glasgow G4 0BA, UK;
Department of Orthopaedics and Sports Medicine,
University of Washington,
Seattle, WA 98195

James Woodburn
Institute of Applied Health Research,
Glasgow Caledonian University,
Glasgow G4 0BA, UK

Sylvain Carbes
Anybody Technology,
Aalborg 9220, Denmark

Detailed knowledge of the loading conditions within the human body is essential for the development and optimization of treatments for disorders and injuries of the musculoskeletal system. While loads in the major joints of the lower limb have been the subject of extensive study, relatively little is known about the forces applied to the individual bones of the foot. The objective of this study was to use a detailed musculoskeletal model to compute the loads applied to the metatarsal bones during gait across several healthy subjects. Motion-captured gait trials and computed tomography (CT) foot scans from four healthy subjects were used as the inputs to inverse dynamic simulations that allowed the computation of loads at the metatarsal joints. Low loads in the metatarsophalangeal (MTP) joint were predicted before terminal stance, however, increased to an average peak of 1.9 times body weight (BW) before toe-off in the first metatarsal. At the first tarsometatarsal (TMT) joint, loads of up to 1.0 times BW were seen during the early part of stance, reflecting tension in the ligaments and muscles. These loads subsequently increased to an average peak of 3.0 times BW. Loads in the first ray were higher compared to rays 2–5. The joints were primarily loaded in the longitudinal direction of the bone. [DOI: 10.1115/1.4032413]

[1]Corresponding author.
Manuscript received May 3, 2015; final manuscript received December 20, 2015; published online January 29, 2016. Assoc. Editor: Kenneth Fischer.

Introduction

While studies of the dynamic loading in major joints, such as the knee [1,2], shoulder [3], and the hip [4], are well established, the forces acting on the bones, ligaments, and muscles of the foot have received much less attention [5,6].

Among foot injuries and diseases, the first metatarsal is one of the most common bones requiring surgery [7]. To improve our understanding of the biomechanical effects of surgeries of the metatarsals and to effectively aid in planning the procedures, it is important to know the loading conditions within the foot. While it is relatively easy to measure overall ground reaction forces generated during gait, it is considerably more difficult to accurately determine the loading of individual foot bones. The highly invasive nature of in vivo experiments required to obtain this information means that researchers have been limited to cadaver tests [5,8], manual calculations [6,9,10], or computer simulations [11–13].

Recently, a detailed, fully dynamic, multisegment kinematic foot model has been developed [14–16], containing 26 segments representing all the bones in the foot as well as the muscles, ligaments, and joints connecting them. The model utilizes inverse dynamics to compute internal forces for all joints, ligaments, and muscles for subject-specific anatomies and recorded motions [14–16]. The objective of this study was to demonstrate the utility of this musculoskeletal foot model to analyze loading of the metatarsal joints during gait for different subjects. We focused on determining dynamic joint loading at the MTP and the TMT joints.

Materials and Methods

Participants. Four healthy male participants underwent barefoot instrumented gait analysis. Average age of the participants was 40.6 (range: 28.3–45.1), average BW was 79 kg (range: 74–90 kg), and average foot length was 24.6 cm (range: 23–26.2 cm). IRB approval was obtained and participants gave informed consent prior to enrolment [15,16].

Data Collection and Processing. The protocol used to obtain the data for this study has been described in detail previously [15,16]. In brief, three walking trials at a self-selected speed per subject were recorded using a 12 camera motion capture system (Oqus 3; Qualisys AB, Gothenburg, Sweden) and a marker protocol with 43 markers on the lower limb [16]. Synchronized ground reaction forces were recorded using force plates embedded within the walkway (9286B; Kistler Instrumente AG, Winterthur, Switzerland), and plantar pressure distributions were recorded using pressure plates (0.5 m length; RSScan International NV, Paal, Belgium). All gait trials were normalized to percent of the gait cycle; only the stance phase was analyzed for this study (0–60% gait cycle, representing heel strike to toe-off). CT scans (1 mm slice thickness) of the feet were taken and subsequently segmented to obtain bone morphology and shape of the participant's feet.

Model. The ANYBODY MODELING SYSTEM V6.0 (AnyBody Technology, Aalborg, Denmark) [17] including the Glasgow–Maastricht foot model [14,15] was used for this investigation. Briefly, each subject-specific model consists kinematically of 36 segments representing the trunk, lumbar vertebras, pelvis, femur, and tibia, and 26 individual segments representing the foot. Trunk and leg segments were scaled according to the overall height of each subject; a nonlinear scaling technique was used to morph the generic model of each individual bone in the foot to the respective CT scan. Segments are connected via kinematic rhythms, constraints, and joints of type revolute, universal, or spherical. The segments are driven according to the recorded motion of the subject in an overdeterminate system, while accounting for skin motion relative to the segments [18].

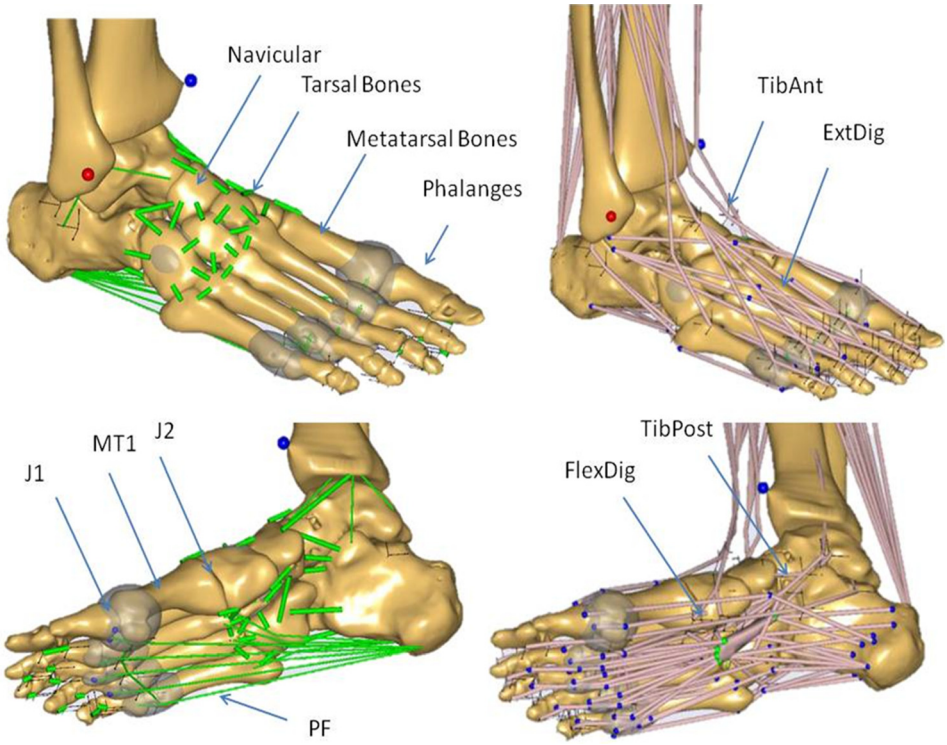

Fig. 1 The Glasgow–Maastricht foot model with bones, major muscles (right side), ligaments (left side), and joints. The first metatarsal bone (MT1) with the MTP joint (J1) and the TMT joint (J2) is highlighted separately. Extensor muscles (ExtDig) and tibialis anterior (TibAnt) can be seen on the dorsal side, PF, and flexor muscles (FlexDig), and tibialis posterior (TibPost) can be seen on the plantar side. Note that most of the foot muscles overlap the tarsal region, but do not insert into it.

The measured ground reaction forces and pressures were applied to the foot model on distinctive nodes on the plantar side. For each time frame, the overall force value and direction from the force plates were used. The measured pressure distribution was averaged in 180 distinctive zones and applied to 180 distinctive nodes on the plantar side of the foot.

The model includes muscles in the leg divided into 159 fascicles. Additionally, the model has the following intrinsic foot muscles: abductor hallucis, flexor hallucis brevis medialis and lateralis, adductor hallucis transverse and oblique, abductor digiti minimi, flexor digiti minimi brevis, dorsal interosseous, plantar interosseous, flexor digitorum brevis, lumbricals, quadratus plantar medialis and lateralis, extensor hallucis brevis, and extensor digitorum brevis. All major foot ligaments are implemented in the model based on the literature data including collaterals divided into several subgroups [19–23], as well as deep metatarsal transverse [19,20], plantar fascia (PF) [19,20,24–26], long plantar [19,20], calcaneo cuboid plantar [19,20,27], calcaneo navicular plantar [19,20,28–30], tarsal [11,19,20,23], and phalangeal [19,20] ligaments (Fig. 1).

The standard muscle recruitment solver [17] was used to compute muscle activations and forces for the different gait trials for each of the subject-specific models. For validation of the foot model, electromyography (EMG) measurements of peroneus, biceps femoris, rectus femoris, vastus lateralis, soleus, gastrocnemius lateralis, gastrocnemius medialis, and tibialis anterior were measured and compared to the predicted muscle activation for 11 subjects (four subjects from this study, plus seven additional subjects). The raw EMG data were low-pass filtered with a cut-off frequency of 3 Hz with a fourth-order Butterworth filter in the AnyBody Modeling System in order to get an envelope that describes muscle activity as previously described [31]. The processed EMG data were normalized with respect to the maximum measured EMG value for that muscle over all the measurements. The predicted muscle activity in the model was defined as the muscle force at that particular instant in time divided by the maximal force of that particular muscle. The strength of each muscle in the model was scalable based on the subject's weight and height ("strength scaling" within the modeling system, previously validated for other kinematic models [14,15,17,]). The passive stiffness of the ligaments was validated by comparing load versus displacement curves of the model with published data of an experimental setup of a (passive) cadaveric foot [15].

Metatarsal Loads. In the model, more than 75 forces act on the first metatarsal, including joint reaction, ground reaction (via pressure nodes), muscle, and ligament forces. Three joints connect the first metatarsal with its adjacent bones, including the TMT joint (connecting the medial cuneiform with the metatarsal) and the MTP joint (connecting the metatarsal with the phalanx). These two joints are highly constrained, with motion described as minor gliding in the anatomical literature [32] and in in vivo studies [19,33,34]. Due to the difficulties in measuring the small movements outside of the primary plane of motion using a noninvasive motion capture approach, universal joints were used for these joints in the model. The center of rotation (CoR) for the TMT joint was estimated from the slightly concave joint facet at the base of the first metatarsal. The CoR was placed posterior of the two articulation surfaces, allowing for the gliding motions. The position of the MTP CoR was placed in the center of the corresponding metatarsal head, and the orientation of the axes was positioned in order to allow flexion/extension and abduction/adduction. The third joint in the model associated with the first metatarsal, connecting the first and second metatarsals, was modeled as an ellipsoid joint.

Several muscles act directly or have via nodes on the metatarsal, with most muscles divided into several branches: tibialis

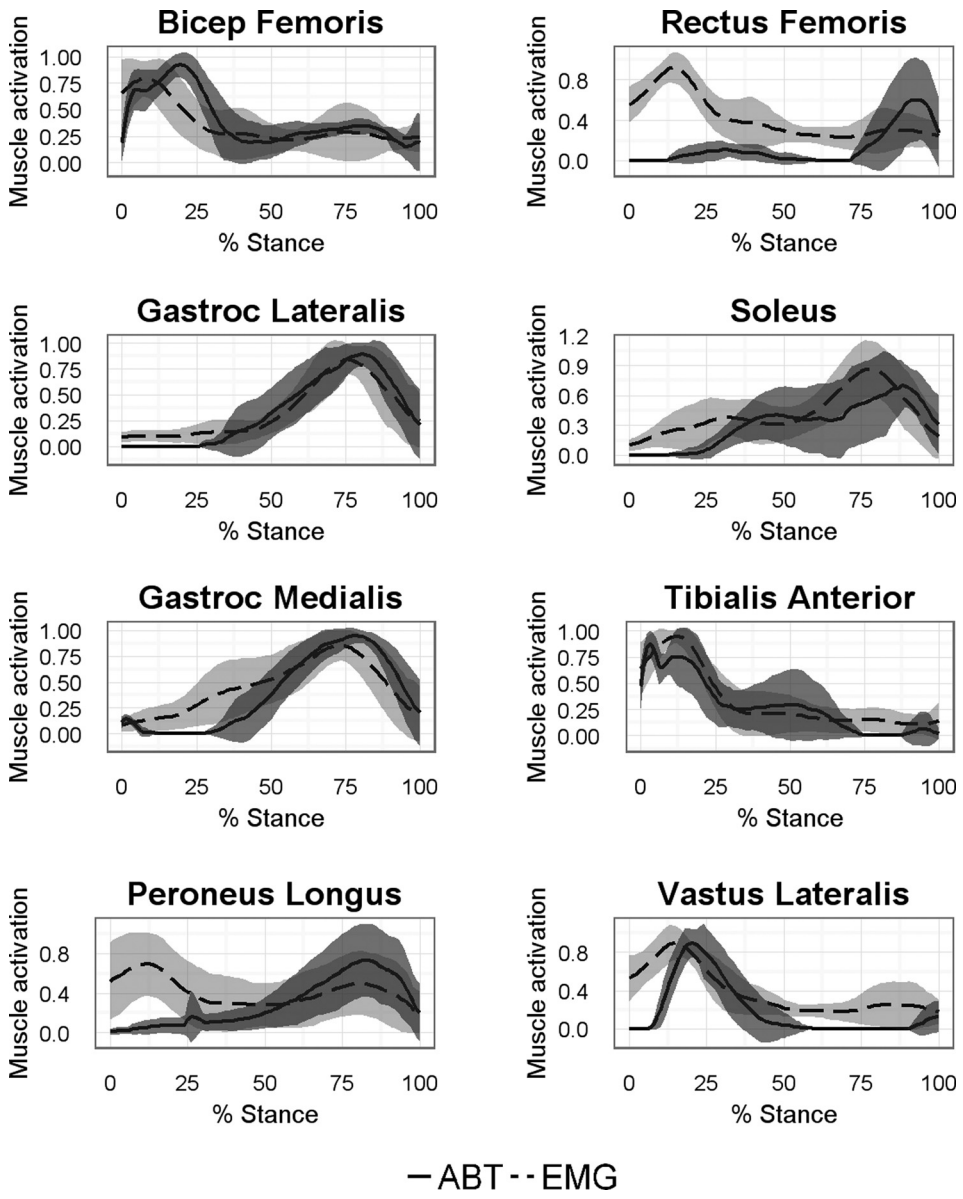

Fig. 2 Comparison of EMG measurements ("EMG") of the peroneus, biceps femoris, rectus femoris, vatus lateralis, soleus, gastrocnemius lateralis, gastrocnemius medialis, and tibialis anterior with predicted muscle activations ("ABT") from the model

anterior, peroneus, flexor hallucis longus, and extensor hallucis longus. Additionally, multiple ligaments were directly attached to the metatarsal in the model: metatarsal transversum profundum, plantar plate (medial and lateral), TMT ligament (dorsal and lateral), and aponeurosis plantaris (Fig. 1).

Metatarsals two to five were modeled in a similar way as the first metatarsal, with joints to the phalanges, adjacent metatarsals, and intermediate cuneiform, lateral cuneiform, or cuboid, respectively.

Joint reaction forces of the MTP joint and TMT joint were computed. All the loads were normalized according to the BW of each subject.

Results

The comparison of the EMG measurements of the peroneus, biceps femoris, rectus femoris, vastus lateralis, soleus, gastrocnemius lateralis, gastrocnemius medialis, and tibialis anterior with predicted muscle activations showed good qualitative agreement with the exception of rectus femoris (Fig. 2).

The resultant joint reaction forces at the first MTP joint showed very low loads in the first third of the gait cycle for each subject (Fig. 3). Subsequently, the force increased until a peak force was reached at about 75% stance phase. The average peak load was measured as $1.9 \times \text{BW} \pm 0.4$.

The resultant joint reaction forces at the first TMT joint showed loads of up to $1 \times \text{BW}$ until 50% of stance, followed by a peak at 80%, for each of the four subjects (Fig. 4). Peak forces at the joint were $3.0 \times \text{BW} \pm 0.56$.

The reaction forces at individual MTP joints, averaged across the four subjects, are presented in Fig. 5. The joint reaction forces for the second to the fifth ray stay at around $0.1–0.2 \times \text{BW}$, over an order of magnitude less than for the first ray.

The reaction forces at individual TMT joints, averaged across the four subjects, are presented in Fig. 6. The joint in ray 2 between the intermediate cuneiform and the second metatarsal bone, as well as the joint in ray 3 between the lateral cuneiform and the third metatarsal bone, had average peak loads of approximately $1 \times \text{BW}$ at around 75% of stance. The TMT joints in the fourth and fifth ray, between the cuboid and fourth and fifth

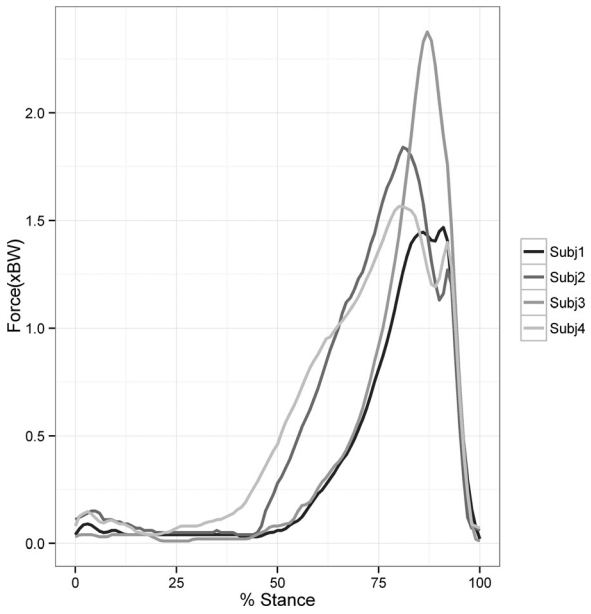

Fig. 3 First MTP joint reaction force during stance phase in each of the four subjects

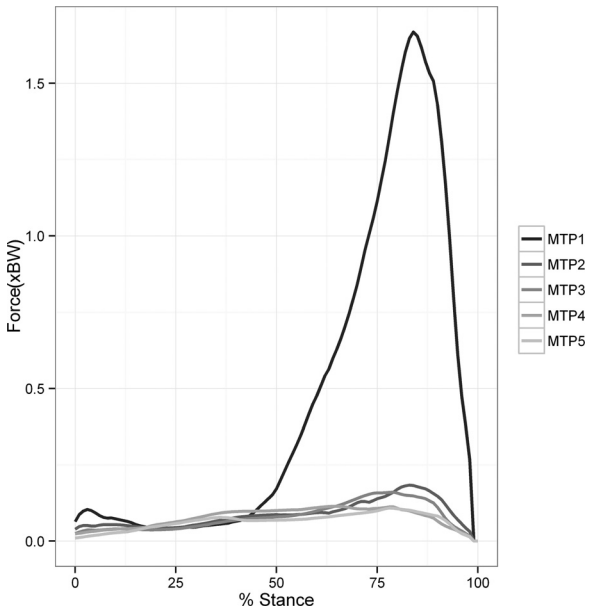

Fig. 5 Joint reaction forces of all the five MTP joints during stance as average of four different subjects

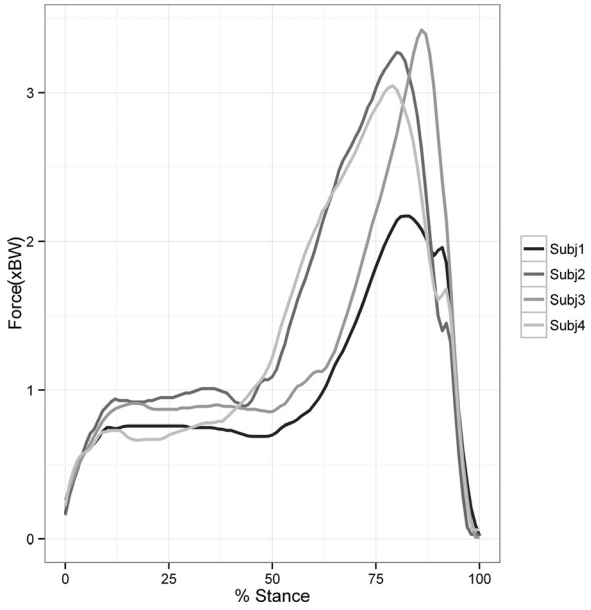

Fig. 4 First TMT joint reaction force during the gait cycle in each of the four subjects

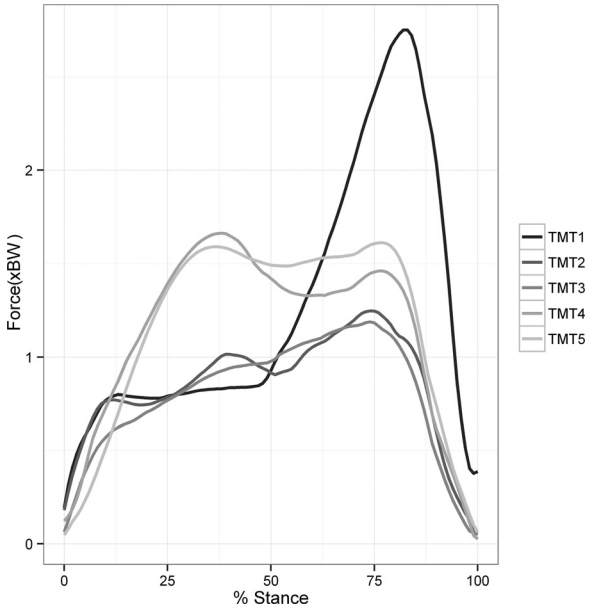

Fig. 6 Joint reaction forces of all the five TMT joints during stance as average of four different subjects

metatarsals, respectively, had average peak loads of approximately $1.5 \times$ BW sustained across approximately 30% of the gait cycle.

The peak forces in the first ray of the TMT and MTP joints are shown in Table 1. The longitudinal (axial) component is the main contributor for the reaction force in the joints.

Table 1 Loads in the first ray of the TMT and MTP joints divided into longitudinal, mediolateral, and plantodorsal components

	Longitudinal	Mediolateral	Plantodorsal	Resultant
TMT ($\times$ BW)	1.67 ± 0.36	0.81 ± 0.16	0.29 ± 0.20	1.90 ± 0.38
MTP ($\times$ BW)	2.96 ± 0.56	0.25 ± 0.05	0.22 ± 0.07	2.98 ± 0.56

Discussion

Increased understanding of the biomechanical loading across bones and joints in the foot can facilitate the development and testing of surgical and nonsurgical treatments for injuries and diseases of the foot [7]. In this study, we have demonstrated the utility of a musculoskeletal model to determine the loads across the MTP and TMT joints of healthy subjects.

Four subjects were analyzed during gait with subject-specific input from motion capture recordings and bone geometry taken from CT scans. The results from the individual subjects follow similar profiles, indicating that these patterns of dynamic loading are characteristic for healthy subjects. Peak forces across the MTP

and TMT joints, occurring around toe-off in the gait cycle, are likely the result of the full BW passing through the forefoot as well as the muscle forces required to stabilize the posture. High muscle and ligament forces are necessary to transfer the loads from an initial horizontal direction to the center of pressure under the toes as the gait cycle approaches toe-off. The computed resultant forces include both axial (longitudinal) and shear components though the dominant forces are in the longitudinal direction of the first metatarsal bone. The shear force was seen to be relatively small for the majority of the gait cycle indicating that the force is primarily transferred straight through the metatarsal with minimal bending.

Stokes et al., Jacob, and Kirane et al. reported peak forces of $0.8–0.9 \times$ BW in the first metatarsal joint and $1.2 \times$ BW in the first metatarsal head [6,13,35]. These loads are low compared to our findings, especially considering that the full ground reaction force is usually applied via the big toe to the first metatarsal at the end of the stance phase, and ground reaction forces show values during this time point of about $1.1 \times$ BW. Combined with forces from muscles stabilizing the joint, this current study predicts $1.5–2 \times$ BW loads in the metatarsal joint. In order to transfer the vertical ground reaction force into the direction of the metatarsal axis, several muscles and ligaments will be activated, as reflected in the joint loading between the medial cuneiform and first metatarsal.

Based on the predicted loads in both the TMT and MTP joints for the four subjects examined here, load is primarily transferred through the first metatarsal, as compared to the other rays, with the loads more evenly distributed across the TMT joints than the MTP joints. The predicted values compare well with the cadaveric simulations by Sharkey et al. [36], who measured the axial load on the second metatarsal at late terminal stance to be on average > 800 N. Loads of this magnitude are in line with our measurements, assuming the cadaveric loading is on average representative of a 70–75 kg person. A full line of cadaveric experiments from Sharkey et al. showed similar results for metatarsal loads [8,36,37].

Musculoskeletal models enable investigation of natural processes that cannot be explored easily with in vitro or in vivo experiments, and the 26 segment foot model used in this study is currently the most detailed and advanced foot model available. Nevertheless, proper appreciation of the limitations of the model is important to ensure appropriate use of the results and predictions presented here. First, the sample size of four subjects is not expected to fully represent normal anatomical variation. For this reason, no statistical assessments of model results are presented here, but rather, results are intended as illustrative of a methodology that may be more fully built out in subsequent work with additional specimens. Additionally, all four models utilized here represent healthy patients, and thus, the extensibility of the results here to pathologic diseases or conditions of the foot (e.g., flatfoot, hallux valgus, and metatarsalgia) that require biomechanical intervention should be done cautiously. Third, the modeling framework utilized here is based on rigid body simulation, which has the benefit of including the complexity of the whole body while still being an efficient simulation, but translation of the loads predicted here to heterogeneous stress or strain in constituent bodies requires more detailed analysis, such as finite-element analysis [38,39]. Finally, though EMG measurements generally compare favorably to model predictions of muscle activity shown here, there are no direct measurements of muscle activity in the vicinity of the metatarsals, and thus, the application here represents a reasonable but nevertheless an extrapolation of the model as validated.

Conclusion

In this study, we have demonstrated the utility of a novel musculoskeletal foot model for providing detailed insights into the loading on the metatarsal joints and indicate that peak axial loads of around three times BW may be experienced during gait.

Acknowledgment

The data were acquired as part of the A-FOOTPRINT Project,[2] funded through the European Commission Seventh Framework Programme (Grant No. NMP2-SE-2009-228893). Additional funding was given by Zimmer, Inc., Warsaw, IN.

References

[1] D'Lima, D. D., Fregly, B. J., Patil, S., Steklov, N., and Colwell, C. W., 2012, "Knee Joint Forces: Prediction, Measurement, and Significance," Proc. Inst. Mech. Eng., Part H, **226**(2), pp. 95–102.
[2] Kutzner, I., Heinlein, B., Graichen, F., Bender, A., Rohlmann, A., Halder, A., Beier, A., and Bergmann, G., 2010, "Loading of the Knee Joint During Activities of Daily Living Measured In Vivo in Five Subjects," J. Biomech., **43**(11), pp. 2164–2173.
[3] Bergmann, G., Graichen, F., Bender, A., Kääb, M., Rohlmann, A., and Westerhoff, P., 2007, "In Vivo Glenohumeral Contact Forces—Measurements in the First Patient 7 Months Postoperatively," J. Biomech., **40**(10), pp. 2139–2149.
[4] Bergmann, G., Deuretzbacher, G., Heller, M., Graichen, F., Rohlmann, A., Strauss, J., and Duda, G. N., 2001, "Hip Contact Forces and Gait Patterns From Routine Activities," J. Biomech., **34**(7), pp. 859–871.
[5] Kirane, Y. M., Michelson, J. D., and Sharkey, N. A., 2008, "Contribution of the Flexor Hallucis Longus to Loading of the First Metatarsal and First Metatarsophalangeal Joint," Foot Ankle Int., **29**(4), pp. 367–377.
[6] Jacob, H. A., 2001, "Forces Acting in the Forefoot During Normal Gait—An Estimate," Clin. Biomech. (Bristol, Avon), **16**(9), pp. 783–792.
[7] Cracchiolo, A., 3rd, Swanson, A., and Swanson, G. D., 1981, "The Arthritic Great Toe Metatarsophalangeal Joint: A Review of Flexible Silicone Implant Arthroplasty From Two Medical Centers," Clin. Orthop. Relat. Res., **157**, pp. 64–69.
[8] Sharkey, N. A., Ferris, L., Smith, T. S., and Matthews, D. K., 1995, "Strain and Loading of the Second Metatarsal During Heel-Lift," J. Bone Jt. Surg. Am., **77**, pp. 1050–1057.
[9] Stokes, I., Hutton, W., and Stott, J. R., 1979, "Forces Acting on the Metatarsals During Normal Walking," J. Anat., **129**(3), pp. 579–590.
[10] Wyss, U. P., McBride, I., Murphy, L., Cooke, T. D., and Olney, S. J., 1990, "Joint Reaction Forces at the First MTP Joint in a Normal Elderly Population," J. Biomech., **23**(10), pp. 977–984.
[11] Cheung, J. T.-M., Zhang, M., Leung, A. K.-L., and Fan, Y.-B., 2005, "Three-Dimensional Finite Element Analysis of the Foot During Standing—A Material Sensitivity Study," J. Biomech., **38**(5), pp. 1045–1054.
[12] Liacouras, P. C., and Wayne, J. S., 2007, "Computational Modeling to Predict Mechanical Function of Joints: Application to the Lower Leg With Simulation of Two Cadaver Studies," ASME J. Biomech. Eng., **129**(6), pp. 811–817.
[13] Wu, L., 2007, "Nonlinear Finite Element Analysis for Musculoskeletal Biomechanics of Medial and Lateral Plantar Longitudinal Arch of Virtual Chinese Human After Plantar Ligamentous Structure Failures," Clin. Biomech. (Bristol, Avon), **22**(2), pp. 221–229.
[14] Carbes, S., Telfer, S. T. S., Woodburn, J., Oosterwaal, M., and Rasmussen, J., 2011, "A New Multisegmental Foot Model and Marker Protocol for Accurate Simulation of the Foot Biomechanics During Walking," Congress of the International Society of Biomechanics (ISB 2011), Brussels, Belgium, July 3–7, Paper No. 183.
[15] Carbes, S., Tørholm Christensen, S., and Rasmussen, J., 2011, "A Detailed Twenty-Six Segments Kinematic Foot Model for Biomechanical Simulation," A-FOOTPRINT (Ankle and Foot Orthotic Personalisation Via Rapid Manufacturing) Project, Funded by the European Commission Seventh Framework Programme, Glasgow Caledonian University, Glasgow, UK.
[16] Oosterwaal, M., Telfer, S., Tørholm Christensen, S., Carbes, S., van Rhijn, L., Macduff, R., Meijer, K., and Woodburn, J., 2011, "Generation of Subject-Specific, Dynamic, Multisegment Ankle and Foot Models to Improve Orthotic Design: A Feasibility Study," BMC Musculoskeletal Disord., **12**(1), pp. 256–266.
[17] Rasmussen, J., Damsgaard, M., and Voigt, M., 2001, "Muscle Recruitment by the Min/Max Criterion—A Comparative Numerical Study," J. Biomech., **34**(3), pp. 409–415.
[18] Andersen, M. S., Damsgaard, M., MacWilliams, B., and Rasmussen, J., 2010, "A Computationally Efficient Optimisation-Based Method for Parameter Identification of Kinematically Determinate and Over-Determinate Biomechanical Systems," Comput. Methods Biomech. Biomed. Eng., **13**(2), pp. 171–183.
[19] Lundgren, P., Nester, C., Liu, A., Arndt, A., Jones, R., Stacoff, A., Wolf, P., and Lundberg, A., 2008, "Invasive In Vivo Measurement of Rear-, Mid- and Forefoot Motion During Walking," Gait Posture, **28**(1), pp. 93–100.
[20] Cailliet, R., 2004, *The Illustrated Guide to Functional Anatomy of the Musculoskeletal System*, D J R Evans, AMA Press, Chicago, IL.

[2] www.afootprint.eu

[21] Stagni, R., Leardini, A., and Ensini, A., 2004, "Ligament Fibre Recruitment at the Human Ankle Joint Complex in Passive Flexion," J. Biomech., **37**(12), pp. 1823–1829.
[22] Funk, J. R., Hall, G. W., Crandall, J. R., and Pilkey, W. D., 2000, "Linear and Quasi-Linear Viscoelastic Characterization of Ankle Ligaments," ASME J. Biomech. Eng., **122**(1), pp. 15–22.
[23] Siegler, S., Udupa, J. K., Ringleb, S. I., Imhauser, C. W., Hirsch, B. E., Odhner, D., Saha, P. K., Okereke, E., and Roach, N., 2005, "Mechanics of the Ankle and Subtalar Joints Revealed Through a 3d Quasi-Static Stress MRI Technique," J. Biomech., **38**(3), pp. 567–578.
[24] Moraes do Carmo, C. C., Fonseca de Almeida Melão, L. I., Valle de Lemos Weber, M. F., Trudell, D., and Resnick, D., 2008, "Anatomical Features of Plantar Aponeurosis: Cadaveric Study Using Ultrasonography and Magnetic Resonance Imaging," Skeletal Radiol., **37**(10), pp. 929–935.
[25] Wright, I., Neptune, R., van Den Bogert, A., and Nigg, B., 1998, "Passive Regulation of Impact Forces in Heel-Toe Running," Clin. Biomech. (Bristol, Avon), **13**(7), pp. 521–531.
[26] Kitaoka, H. B., Luo, Z. P., Growney, E. S., Berglund, L. J., and An, K. N., 1994, "Material Properties of the Plantar Aponeurosis," Foot Ankle Int., **15**(10), pp. 557–560.
[27] Ward, K. A., and Soames, R. W., 1997, "Morphology of the Plantar Calcaneocuboid Ligaments," Foot Ankle Int., **18**(10), pp. 649–653.
[28] Taniguchi, A., Tanaka, Y., Takakura, Y., Kadono, K., Maeda, M., and Yamamoto, H., 2003, "Anatomy of the Spring Ligament," J. Bone Jt. Surg. Am., **85-A**, pp. 2174–2178.
[29] Patil, V., Ebraheim, N. A., Frogameni, A., and Liu, J., 2007, "Morphometric Dimensions of the Calcaneonavicular (Spring) Ligament," Foot Ankle Int., **28**(8), pp. 927–932.
[30] Mengiardi, B., Zanetti, M., Schöttle, P. B., Vienne, P., Bode, B., Hodler, J., and Pfirrmann, C. W. A., 2005, "Spring Ligament Complex: MR Imaging-Anatomic Correlation and Findings in Asymptomatic Subjects," Radiology, **237**(1), pp. 242–249.
[31] de Zee, M., Dalstra, M., Cattaneo, P. M., Rasmussen, J., Svensson, P., and Melsen, B., 2007, "Validation of a Musculo-Skeletal Model of the Mandible and Its Application to Mandibular Distraction Osteogenesis," J. Biomech., **40**(6), pp. 1192–1201.
[32] Magee, D. J., 1997, *Orthopedic Physical Assessment*, 3rd ed., W.B. Saunders, Philadelphia, PA.
[33] Winson, I., Lundberg, A., and Bylund, C., 1995, "The Pattern of Motion of the Longitudinal Arch of the Foot," Foot, **4**(3), pp. 151–154.
[34] Arndt, A., Wolf, P., Liu, A., Nester, C., Stacoff, A., Jones, R., Lundgren, P., and Lundberg, A., 2007, "Intrinsic Foot Kinematics Measured In Vivo During the Stance Phase of Slow Running," J. Biomech., **40**(12), pp. 2672–2678.
[35] McBride, I. D., Wyss, U. P., Cooke, T. D., Murphy, L., Phillips, J., and Olney, S. J., 1991, "First Metatarsophalangeal Joint Reaction Forces During High-Heel Gait," Foot Ankle, **11**(5), pp. 282–288.
[36] Sharkey, A., Donahue, S. W., and Ferris, L., 1999, "Biomechanical Consequences of Plantar Fascial Release or Rupture During Gait. Part II: Alterations in Forefoot Loading," Foot Ankle Int., **20**(2), pp. 86–96.
[37] Sharkey, N. A., and Hamel, A. J., 1998, "A Dynamic Cadaver Model of the Stance Phase of Gait: Performance Characteristics and Kinetic Validation," Clin. Biomech. (Bristol, Avon), **13**(6), pp. 420–433.
[38] Wong, D. W., Zhang, M., Yu, J., and Leung, A. K. L., 2014, "Biomechanics of First Ray Hypermobility: An Investigation on Joint Force During Walking Using Finite Element Analysis," Med. Eng. Phys., **36**(11), pp. 1388–1393.
[39] Kristen, K. H., Berger, K., Berger, C., Kampla, W., Anzböck, W., and Weitzel, S. H., 2005, "The First Metatarsal Bone Under Loading Conditions: A Finite Element Analysis," Foot Ankle Clin., **10**(1), pp. 1–14.